

Supporting Information

Enhanced Polysulfides Adsorption and Conversion on FeS₂@CNF Modified Separator for Li-S Batteries

Daming Li,^a Yuzheng Li,^a Chengxiao Xu,^a Shuaiquan Zhao,^a Yuchen Zhang,^a Peipei Huo,^{*a}

^a School of Physics and Optoelectronic Engineering, Shandong University of Technology, Xincun West Road 266, Zibo 255000, China;

* Corresponding authors. *E-mail* addresses: peipeihuo@sdut.edu.cn (P. Huo).

Experimental

1. Materials

1,2-Dimethoxyethane (DME, $C_4H_{10}O_2$, 99.9%), 1,3-Dioxolane(DOL, $C_3H_6O_2$, 99.9%), Polyvinylidene fluoride (PVDF, $(C_2H_2F_2)_n$) were purchased from Duoduo Chemical Reagent Co. in Suzhou, China. Ferric chloride ($FeCl_3 \cdot 6H_2O$, AR, 99 %), Sodium chloride (NaCl, AR), polyacrylonitrile (PAN, $(C_3H_3N)_n$), Sulfur (S, AR 99.98%), and n,n-dimethylformamide (DMF, C_3H_7NO , AR, 99.5%) were purchased from Shanghai Aladdin Biochemical Technology Co. The above reagents do not require further purification and all compounds were used immediately.

2. Synthesis of $FeS_2@CNF$

PAN nanofibers were prepared by electrospinning. First, 1.5g PAN powder was dissolved in 8 mL DMF solvent and magnetically stirred for 12h to form a uniform viscous solution. Transfer the viscous solution to a 10 mL syringe and connect it with a 21-gauge needle. The electrospinning parameters were set as follows: the distance between the needle and the fluid collector was 15.5 cm, the voltage was set to 19 kV, and the advancing speed was 0.1 mm min⁻¹. During the electrospinning process, the temperature is maintained at 25 degrees Celsius and the relative humidity at 38%. The PAN nanofibers were cut into sheets and pre-oxidized at 250°C for 2h. In N_2 atmosphere, the pre-oxidized PAN was carbonized at 800°C for 2h to obtain CNF.

CNF was placed in a mixture of $FeCl_3$ and NaCl and stood at 60°C for 12h. Wash with deionized water for many times and dry under vacuum at 25°C to obtain $FeOOH@CNF$. Then, $FeOOH@CNF$ and S powder were mixed at a mass ratio of 1:4 and heated to 350°C in N_2 atmosphere for 2h to obtain the final product $FeS_2@CNF$. The preparation methods for FeS_2 followed the same procedure as described above, except that CNF was omitted.

3. Synthesis of $FeS_2@CNF$ modified separator

Initially, the sample ($FeS_2@CNF$), carbon black, and binder (polyvinylidene fluoride, PVDF) were dispersed in an appropriate amount of N-methylpyrrolidone (NMP) in a mass ratio of 7:2:1. The mixture was ground in a mortar for over 30 mins until a homogeneous slurry was achieved. This slurry was then applied to a commercial PP separator (Celgard-2400) using a spatula with 100-micron scale, resulting in the fabrication of a modified separator, denoted as $FeS_2@CNF//PP$. The modified separators were dried overnight in a vacuum oven at 40°C and then cut into discs with a diameter of 19.0 mm. The average load mass of the active material on the upper surface of the modified diaphragm is 0.45 mg cm⁻².

4. Materials Characterization

The samples underwent morphological characterization and elemental mapping analysis using field emission scanning electron microscopy (SEM; FEI, Quantum 250) and transmission electron microscopy (TEM; JEOL, JEM-2100F). The crystalline phase of $FeS_2@CNF$ was analyzed by X-ray diffraction

(XRD, Panalytical Empyrean). X-ray photoelectron spectroscopy (XPS, Shimadzu/Kratos AXIS SUPRA+) was employed to ascertain the chemical state of the elements present on the sample surface. A contact angle/surface tension meter (Lauda Scientific LSA100) was utilized to investigate the affinity of the samples for the electrolyte. A UV spectrophotometer (Shimadzu, U-4100) was employed to analyze the concentration change of Li_2S_6 solution after the adsorption of various materials.

5. Visual adsorption test of lithium polysulfides

Li_2S_6 solution was selected as a representative of LiPSs for visual adsorption test. A specific amount of sulfur powder and Li_2S in a molar ratio of 5:1 was dissolved in a mixed solvent of 1,2-dimethoxyethane (DME) and 1,3-dioxolane (DOL) (v/v = 1:1). The resulting solution was stirred at 60°C for 24 h to yield a 0.2 mM Li_2S_6 solution. All procedures were conducted within a glove box. The Li_2S_6 solution was subsequently diluted to 2 mmol L⁻¹. Then, 15 mg of $\text{FeS}_2@\text{CNF}$ and FeS_2 were separately added to 4 mL of Li_2S_6 solution. The mixture was left to stand for 8h to ensure thorough completion of the adsorption process. During this time, the color change of the Li_2S_6 solution was observed. The supernatant of the adsorbed solution was extracted for UV-Vis spectral analysis.

6. Electrochemical measurements

The CR2032 coin cell was assembled in an argon-filled glove box. Commercial lithium metal served as the anode, and modified Celgard 2400 was employed as the separator. The electrolyte comprised a 1.0 M LiTFSI solution (v/v = 1:1) with a 1 wt% LiNO_3 additive. Galvanostatic charge-discharge (GCD) and rate performance tests were conducted using a LAND 2100CT test system, with a voltage range of 1.7 to 2.8 V at various current densities (1C = 1675 mAh g⁻¹). Cyclic voltammetry (CV) and electrochemical impedance spectroscopy (EIS) tests were performed using a CHI760E electrochemical workstation. The voltage range for the CV curve test was 1.7 to 2.8 V, with a scan rate range of 0.1 to 0.5 mV s⁻¹. The frequency range for the EIS test was 0.01 to 10 kHz.

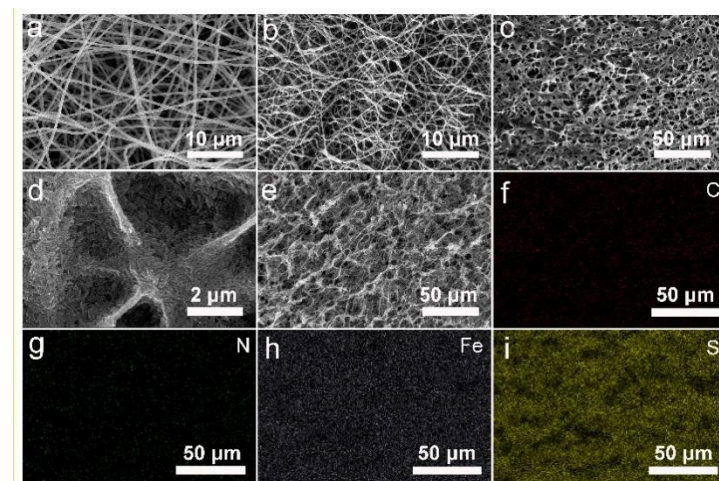


Fig. S1 SEM images of (a) PAN, (b) CNF, (c) and (d) FeOOH@CNF with different magnifications. (e) $\text{FeS}_2@\text{CNF}$ and EDS elemental mapping of C, N, O, Fe, S in $\text{FeS}_2@\text{CNF}$.

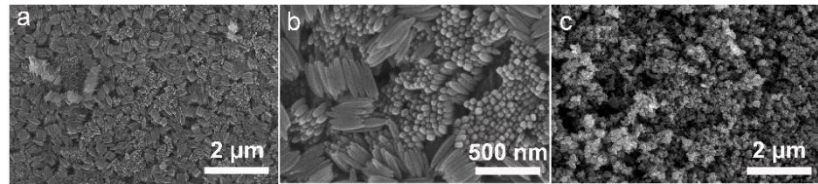


Fig. S2 (a) and (b) SEM images of FeOOH at different magnifications. (c) SEM image of FeS₂.

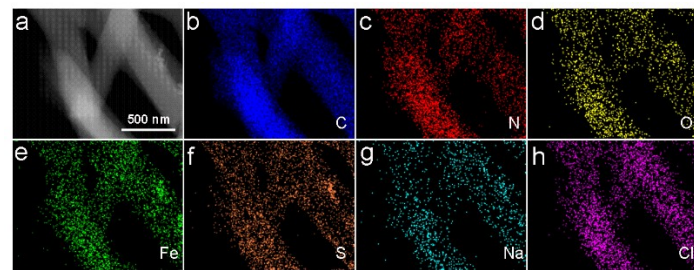


Fig. S3 HAADF-STEM and corresponding areal elemental mapping images of FeS₂@CNF.

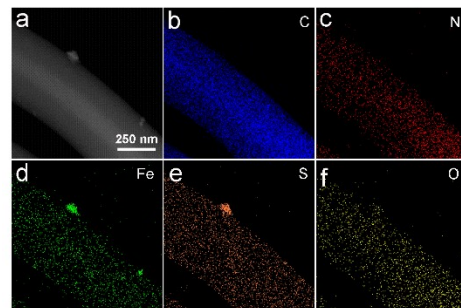


Fig. S4 HAADF-STEM and corresponding areal elemental mapping images of FeS₂@CNF.

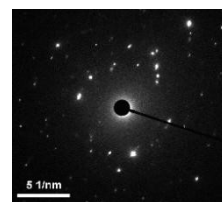


Fig. S5 SAED image of FeS₂@CNF.

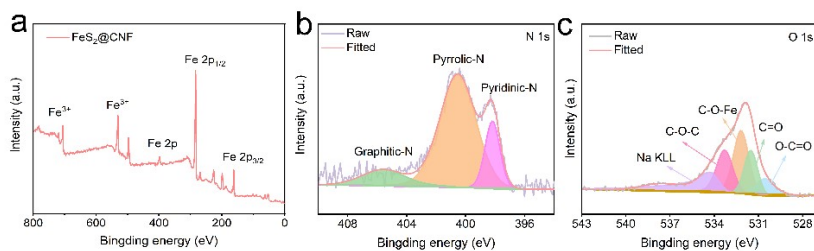


Fig. S6 (a) Total XPS spectra of FeS₂@CNF. (b and c) High-resolution XPS spectra of N 1s, O 1s.

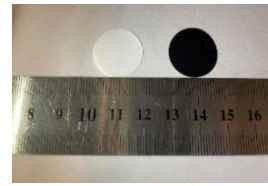


Fig. S7 Digital images of conventional PP separator and $\text{FeS}_2@\text{CNF}/\text{PP}$ separator.

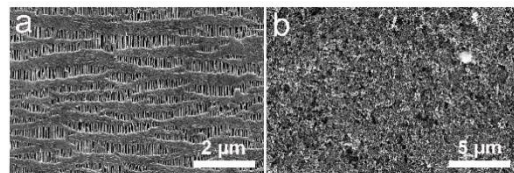


Fig. S8 SEM images of (a) the pristine PP separator, (b) $\text{FeS}_2@\text{CNF}/\text{PP}$ separator.

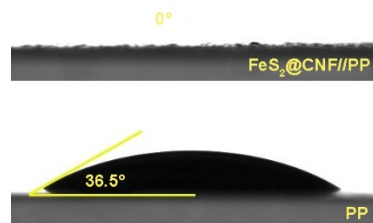


Fig. S9 Contact angles of the pristine PP separator and $\text{FeS}_2@\text{CNF}/\text{PP}$ separator.

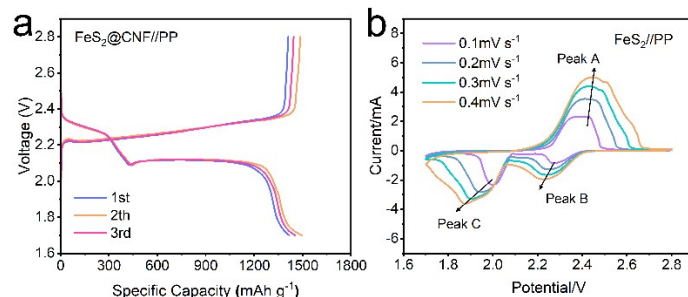


Fig. S10 (a) GCD profiles at 0.1C of $\text{FeS}_2@\text{CNF}/\text{PP}$. (b) CV curves at different scan rates.

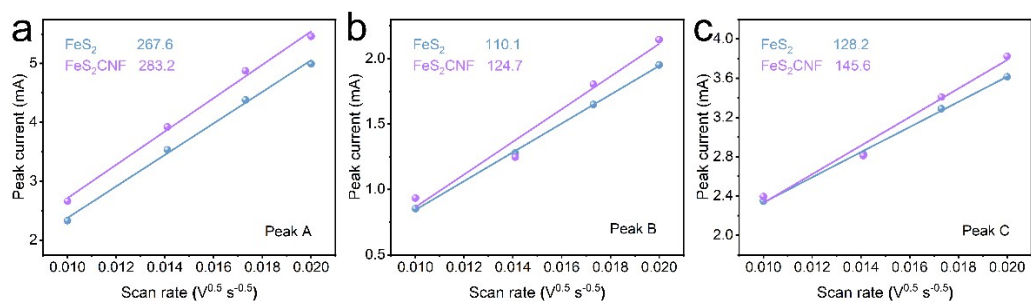


Fig. S11 (a) Relationships between CV peak current and scanning rate.

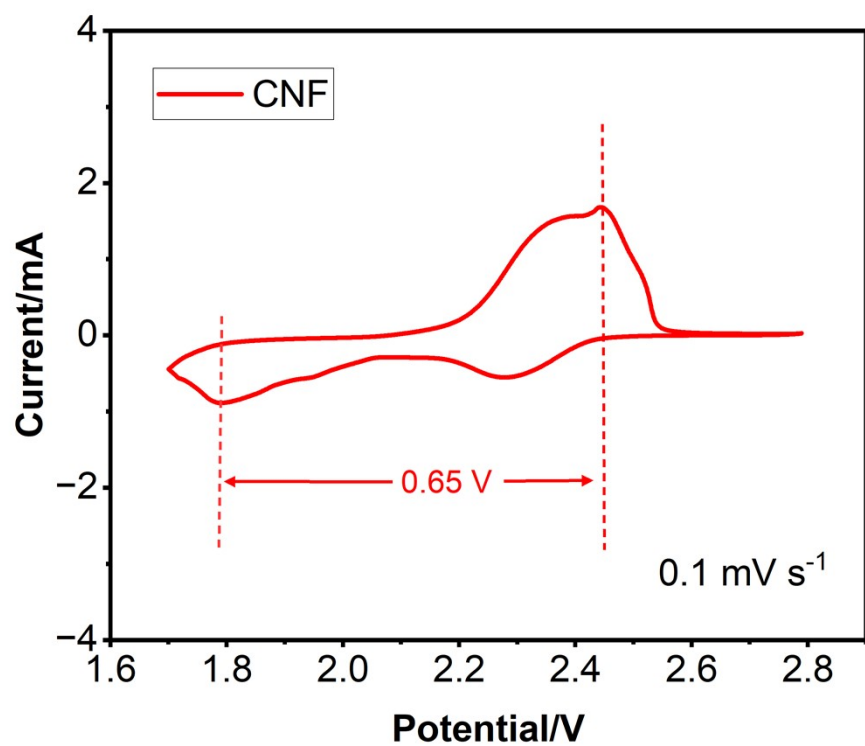


Fig. S12 CV curves of CNF at 0.1 mV s^{-1}

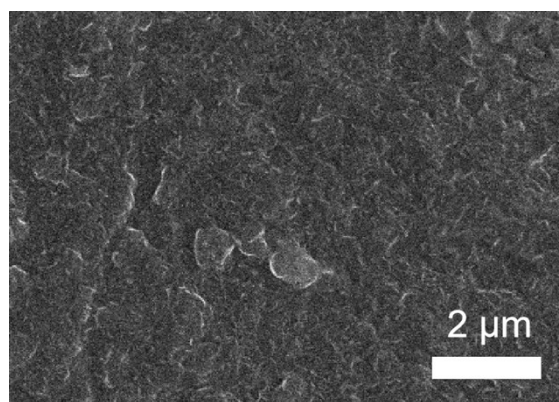


Fig. S13 SEM of lithium sheets after 350 cycles at 0.5 C